Theoretical Notes

Note 200

October 1974

TIME DEPENDENT INTERNAL EMP FOR SPHERICAL AND CYLINDRICAL SYMMETRY

Captain Theodore C. Salvi

Air Force Weapons Laboratory
Kirtland AFB, New Mexico

ABSTRACT

Time varying charge densities and electric fields caused by the symmetric inward emission of electrons are computed for the interior of a hollow sphere and cylinder. The Vlasov equation is derived in circular and cylindrical coordinates. A quasi-static assumption is made. Electric fields are computed at the end of each time step.

Several different methods of obtaining the charge density and field at each time step are discussed, all based on tracing characteristic curves of the Vlasov equation. The simplest of these methods is implemented. The distribution is stored in a discretized phase space, and particles are redistributed to phase points at the end of each time step. A coarse grid is used and numerical techniques are designed so as to expend minimal computer resources. A Maxwellian input distribution is assumed and several sample results are presented.

Contents

Contents

List of Figures

List of Symbols

a	Radius of the spherical or cylindrical shell
C_n	Normalizing constant
e	Charge on electron
ξ	Electric field
E	Total energy
f	Distribution function inside vessel
f_a	Spatial distribution function at a used as boundary condition
f_i	Input distribution function (input per unit time)
I	Intensity of emission from surface (amp/m^2)
$J\left\{\frac{x_1,\ldots,x_n}{y_1,\ldots,y_n}\right\}$	Jacobian relating volume elements
m	Mass: only electron mass used
T	Equivalent temperature of the input distribution
v	Total velocity
v_j	Generalized velocity associated with coordinate j
V	Potential energy for electrons
$\cdot$	Vector dot product; scalar multiplication
$\times$	Vector cross product multiplication

Note: MKS units are used exclusively in this thesis.

TIME DEPENDENT INTERNAL ELECTROMAGNETIC PULSE FOR SPHERICAL AND CYLINDRICAL SYMMETRY

I. Introduction

Since the development of ballistic missiles and military satellites, scientists at the Air Force Weapons Laboratory (AFWL) have been studying the potential effects of a nuclear burst above the earth's atmosphere. One effect is the Electromagnetic Pulse (EMP), a strong transient electromagnetic wave produced by the interaction of gamma rays and x-rays from the burst with the top of the atmosphere (Ref 6). A second effect is the electric potential and space charge produced by the interaction of the gamma rays and x-rays directly with a space vehicle itself. This latter effect is known a System Generated Electromagnetic Pulse (SGEMP), or Internal Electromagnetic Pulse (IEMP).

Background

Work is currently in progress to develop a model which gives an estimate of the magnitude of the IEMP effect, and an indication of how it varies with different parameters. Recent results include solutions to the problem of emission from a flat surface (Ref 5), outward emission from a sphere (Ref 3), and inward emission from a sphere and cylinder (Ref 9). A major limitation of these treatments is the assumption that all electrons are emitted normal to the surface.

The most recent development is the inclusion of an angular distribution in electron emission. This was done by Dr. Donn G.

Shankland of the Air Force Institute of Technology. Shankland addressed the problem of steady-state symmetric emission from a sphere (Ref 8). This thesis is a direct offshoot of his work.

Problem Statement

The problem to be done here is to find the charge density and electric field caused by inward emission with an angular velocity distribution. Both spherically and cylindrically symmetric geometries will be done for both the steady-state and time-dependent cases. The theoretical basis for the solution and possible methods of attack will be discussed. Then the simplest method will be used to generate results to the time-dependent problem.

Theoretical Basis

The electron density is defined by a distribution function in phase space. The motion of electrons in the phase space is described by the Vlasov equation, a form of the Boltzman transport equation with no collisions and only electromagnetic forces present. The electromagnetic fields are themselves caused by the electron distribution, and the Vlasov equation must be solved simultaneously with Maxwell's Equations.

Assumptions

The complete Vlasov equation is a seven-dimensional, quasi-linear, first-order partial differential equation which can in principle be solved by tracing characteristic curves. However, storing a seven-

dimensional array or integrating over a six-dimensional surface requires enormous computer facilities which are not available for this project. The following assumptions are made both to keep the physics simple and to reduce the problem to no more than four dimensions.

(a) The cylinder is infinitely long and both the cylinder and sphere are perfectly evacuated.

(b) The distribution function, f, is independent of the two ignorable coordinates; θ and ϕ in the spherical case and θ and z in the cylindrical case.

(c) Electrons are produced at the surface of the vessel with a known velocity spectrum. The velocities are not necessarily radial in direction but the velocity spectrum is independent of the ignorable coordinates, and symmetric with respect to the surface normal.

(d) All electrons are nonrelativistic.

(e) There are no collisions inside the cavity.

(f) The only force acting on an electron is the electrostatic force caused by the charge distribution of the other electrons.

Assumptions (a) and (b) define the restricted problem that is being solved. While no real-world situation will exactly fit this model, solving this problem gives insight into the more complicated situation. Assumption (c) states that the electron flux at the surface is a known boundary condition of the problem. To be compatible with assumption (b), this distribution must also be independent of θ and ϕ or z. This is not a totally realistic assumption since the most important electron production mechanisms, Compton and photoelectric emission, strongly favor forward emission (Ref 3:39-49).

Most electrons will be created with a velocity moving away from the photon source. But collisions in the material will cause much randomization before they are emitted. Assumption (d) is reasonable for x-ray produced electrons. By assuming the electron velocities are much less than the speed of light, the time of propagation of the electric field can also be ignored. Assumption (e) is justified. Assumption (f) is reasonable for the problem as stated. The symmetry assumed in the problem eliminates system produced magnetic fields, and by assumption there are no background electric or magnetic fields.

Organization

In Chapter 2, basic equations are derived in both spherical and cylindrical coordinates. The assumptions stated above are applied to reduce the problem to its final form. In Chapter 3 the characteristic curves and various methods of applying them are discussed. The simplest method is used to generate numerical results. The numerical method and results are examined in Chapter 4 and 5. Conclusions and recommendations are presented in Chapter 6.

II. Basic Equations

As noted in the introduction, two equations must be solved simultaneously, one transport equation and one field equation. In this Chapter, these equations will be derived in both spherical and cylindrical coordinates. By choosing the proper coordinate system, the Vlasov transport Equation is identical in form for both spherical and cylindrical symmetry. The equations for the electric field are easily derived, but they are different for the two cases.

Vlasov Equation

The Vlasov equation is a special case of the Boltzman transport equation. The Boltzman equation is usually written in vector form as

$$\frac{df}{dt} = \frac{\partial f}{\partial t} + \vec{v}\cdot\vec{\nabla}_r f + \frac{\vec{F}}{m}\cdot\vec{\nabla}_v f \qquad (1)$$

The Vlasov equation is a special case of the Boltzman equation where there are no collisions, therefore $\frac{df}{dt} = 0$, and the only force present is the Lorentz force, $F = q(\vec{E} + \vec{v}\times\vec{B})$.

The Vlasov equation in this form can be directly transformed from rectangular coordinates to any desired coordinate system, but the process is tedious. A much simpler approach is to expand $\frac{df}{dt}$ in terms of partial derivatives. If $f = f(q_1,\ldots,q_j,v_1,\ldots,v_j,t)$, then

$$\frac{df}{dt} = \frac{df}{dt} + \sum_1^j \frac{\partial f}{\partial q_i}\frac{dq_i}{dt} + \sum_1^j \frac{\partial f}{\partial v_i}\frac{dv_i}{dt} \qquad (2)$$

However, there still remains the difficult problem of relating the Lorentz force to the $\frac{dv_i}{dt}$ terms.

Poisson Bracket Notation. The most elegant, yet ultimately the simplest method found for deriving the Vlasov equation in general coordinate systems is by use of the Poisson bracket notation. If the Hamiltonian, H, of the system is not time-dependent, the total derivative of the distribution function can be written as (Ref 4:Ch 8)

$$\frac{df}{dt} = [f,H] + \frac{\partial f}{\partial t} \tag{3}$$

The distribution function, f, is defined in a seven-dimensional space with cannonical coordinates q_i, p_i, and t. The Poisson bracket is defined as

$$[f,H] = \sum_i \left(\frac{\partial f}{\partial q_i}\frac{\partial H}{\partial p_i} - \frac{\partial f}{\partial p_i}\frac{\partial H}{\partial q_i}\right) \tag{4}$$

and the Hamiltonian in this case equals the total energy a particle would have at each point in phase space.

Eq (3) is equivalent to Eq (1) whenever the force can be derived from a time independent potential. If the total energy, $E(q_i,\ldots,q_j,p_i,\ldots,p_j,t)$, is substituted for H in Eq (3) the two are equivalent in all stationary coordinate systems. This method can be used to derive the Boltzman equation in any stationary coordinate system, with the restriction that the coordinate and velocity variables

must be in associated canonical pairs.

There is one further level of sophistication in this formulation of transport theory. If time is considered to be one of the normal mechanical variables of the system, the momentum associated with time is the negative of the total energy (Ref 7:133). In this formulation the phase space is eight-dimensional and the Hamiltonian is identically zero (Ref 7:185). The basic equation now has the even more simple form

$$\frac{df}{dt} = [f,H] \tag{5}$$

This form is used in the derivation below. The new coordinate, -E, is not truly independent. It is the sum of the kinetic and potential energies, both which can be totally specified by the other seven variables. For the moment, it will be useful to treat it as independent.

Derivation of Vlasov Equation. In the cylindrical case the normal cylindrical coordinates, r,θ, and z, are used. The Lagrangian function in these coordinates is

$$\begin{aligned} L &= \text{Kinetic Energy} - \text{Potential Energy} \\ &= \frac{m}{2}(\dot{r}^2+r^2\dot{\theta}^2+\dot{z}^2) - V(r,\theta,z,t) \end{aligned} \tag{6}$$

The Hamiltonian is derived by using $p_i = \frac{\partial L}{\partial \dot{q}_i}$ and $H = \sum p_i\dot{q}_i - L$ with $q_4 = t$ and $p_4 = -E$.

$$H = \frac{1}{2m}(p_r^2 + \frac{p_\theta^2}{r^2}+p_z^2) + V(r,\theta,z,t) - E = 0 \tag{7}$$

Using Eq (7) in Eq (5) together with the assumptions that the potential, V, and the distribution, f, are independent of θ and z, the transport equation is

$$\frac{df(r,p_r,p_\theta,p_z,t,E)}{dt} = \frac{\partial f}{\partial r}\frac{p_r}{m} + \frac{\partial f}{\partial p_r}\left\{\frac{p_\theta^2}{mr^3} + \frac{\partial V}{\partial r}\right\} + \frac{\partial f}{\partial t} + \frac{\partial f}{\partial E}\frac{\partial V}{\partial t} \tag{8}$$

Defining $v_l = p_l/m$ and using the assumptions of the Vlasov equation

$$0 = \frac{\partial f}{\partial t} + \frac{\partial f}{\partial r}v_r + \frac{\partial f}{\partial v_r}\left\{\frac{v_\theta^2}{r^3} - \frac{e\xi}{m}\right\} + \frac{\partial f}{\partial E}\frac{\partial V}{\partial t} \tag{9}$$

where the electric field, $\xi = \frac{1}{e}\frac{\partial V}{\partial r}$, depends on r and t. The velocity along the cylinder axis, v_z, can be integrated out of distribution function

$$f'(r,v_r,v_\theta,t,E) = \int dv_z\, f(r,v_r,v_\theta,v_z,t,E) \tag{10}$$

Further references to the distribution function in cylindrical coordinates assume implicitly that this v_z integration has been done.

In the spherical case the coordinates chosen are r, θ, and ϕ, where θ is chosen in the direction of a particles movement and ϕ orthogonal to it. Thus p_θ is always zero and the Vlasov equation is identical in form to Eq (9).

The variables in Eq (9) are not truly independent. One of the arguments, either r, v_r, v_θ, t, or E, must be dropped from the distribution function. The term of Eq (9) containing the partial

derivative of f with respect to that variable also vanishes. Ususally, the total energy is dropped as a variable. That is the method used in the time-dependent numerical solution in Chapters 4 and 5. In the steady-state solution discussed in Chapter 3, however, it is advantageous to keep E as an independent variable and drop v_r.

Electric Field Equations

Because of the assumed symmetry of the problem, the electric field can be computed easily from Gauss's law. In the cylindrical case

$$\xi(r,t) = \frac{-e}{2\pi\varepsilon_o r} N(r,t) \tag{11}$$

where $N(r,t)$ is the total number of electrons inside a radius r per unit length in the z direction. In the spherical case

$$\xi(r,t) = \frac{-e}{4\pi\varepsilon_o r^2} N(r,t) \tag{12}$$

where $N(r,t)$ is total number of electrons inside r. The potential, $V(r,t)$ is found by integrating $e\xi dr$. Zero potential is assumed either at the origin or at the surface.

Again due to symmetry, no internally produced magnetic fields occur. In the cylindrical case, z and θ magnetic interactions are avoided by requiring that the distribution function is even with respect to v_z and v_θ.

III. Solution by Characteristic Curves

Neglecting the integral nature of the electric field term, the Vlasov equation is a quasi-linear, first order, partial differential equation. The solution of this type of equation can be accomplished by tracing the characteristic curves of the equation. If the distribution function is a function of n independent variables, the solution to the equation is a n-dimensional manifold in an n+1-dimensional space. The characteristic curves are one-parameter lines in this manifold which are traced from the boundary conditions. The boundary conditions must be an n-1-dimensional manifold. The individual characteristic curves are simple to trace, but many curves must be traced to map out the entire solution.

In this Chapter the application of characteristic curves to the IEMP problem is discussed. A short algebraic proof and a three-space geometrical view of characteristics is contained in Appendix A to provide the necessary background for this Chapter. Several methods of attacking the time-dependent problem are discussed. Shankland's work on the steady-state IEMP problem is viewed in relation to the general time-dependent approach.

Application to the Symmetric IEMP Problem

Because of symmetry assumptions, the solution space to be considered is only five-dimensional. The space consists of the dependent variable, f, and four independent variables, r, v_r, v_θ, t. The solution is represented by a four-dimensional hyper-surface in the five-

dimensional solution space. This hyper-surface is found by tracing one-parameter characteristic curves from some given three-dimensional boundary condition. The characteristic curves are obtained by comparing the coefficients of Eq (19) of Appendix A to the coefficients of the Vlasov equation derived in the previous chapter, Eq (9). The result is

$$df:dt:dr:dv_r:dv_\theta:dE :: 0:1:v_r:\frac{v_\theta^2}{r^3}-\frac{e\xi}{m}:0:\frac{\partial V}{\partial t} \qquad (13)$$

Two conditions of Eq (13), $df=0$, and $dv_\theta=0$ reduce the computations necessary to trace an individual characteristic curve. Both conditions are expected for physical reasons: the total number of particles and the angular momentum of a particle are not changed by the transport process. Using the velocity coordinate v_θ as derived from Eq (6), we have $v_\theta=r^2\dot{\theta}=\ell/m$, where ℓ is the angular momentum. Since the force is purely radial this remains constant. But this does not reduce the number of curves necessary; a sufficient number of different characteristic curves must be traced to represent trajectories of particles throughout the angular momentum spectrum.

Special attention must be given to computing the electric field. The electric field is found by integrating the distribution function, f. A quasi-static case is assumed. Particles are moved for some small period of time before a new electric field is found. This forces time to be the basic independent variable used to trace the characteristic curves. To get the total enclosed charge, the distribution function at the desired time is found by tracing characteristic curves. The total enclosed charge inside radius r is then

$$N(r,t) = \int_0^r dr' \int_{-\infty}^{\infty} dv_r \int_{-\infty}^{\infty} dv_\theta \; f(r',v_r,v_\theta,t) \qquad (14)$$

Evaluating this integral for all radii and times is the key to the symmetric IEMP problem. The quantities of ultimate interest, charge density and potential, are easily calculated from $N(r,t)$. Several methods of evaluating the integral of Eq (14) are possible.

Forward Time Step and Store the Distribution

The most straight-forward method available to evaluate Eq (14) is to store the current distribution. This approach was used by the author and specific numerical techniques and results are given in Chapters 4 and 5. The method is basically a particle simulation. All particles are placed in 'bins' in r,v_r,v_θ space and traced along their characteristic trajectories. After all bins are traced for one time-step, the integrations of Eq (14) are done. A new electric field is computed and the particles are traced for another time-step.

The simplest method of storing the distribution function, f, is to store the final r,v_r, and v_θ of each bin of particles. The generalized angular velocity, v_θ, remains constant so it can be stored implicitly by the location in storage. The number of particles in each bin, $f(r,v_r,v_\theta)$, also must be stored. In this type of memory scheme the total computer core necessary for storage of f depends on the number of bins still within the limiting radius of the vessel.

Another method of storing f is to discretize the phase space itself. The phase space is stored as an three-dimensional array. The

coordinates r, v_r, and v_θ are defined by position in the array. The number of particles at those coordinates, $f(r,v_r,v_\theta)$ is placed in that storage position. If a trajectory places a bin of particles between phase points, the particles in the bin are split up between adjacent phase points. Fig. 1 illustrates the different trajectories traced using these two different methods of storing f. This author has used a discretized phase space in the numerical work described in Chapters 4 and 5.

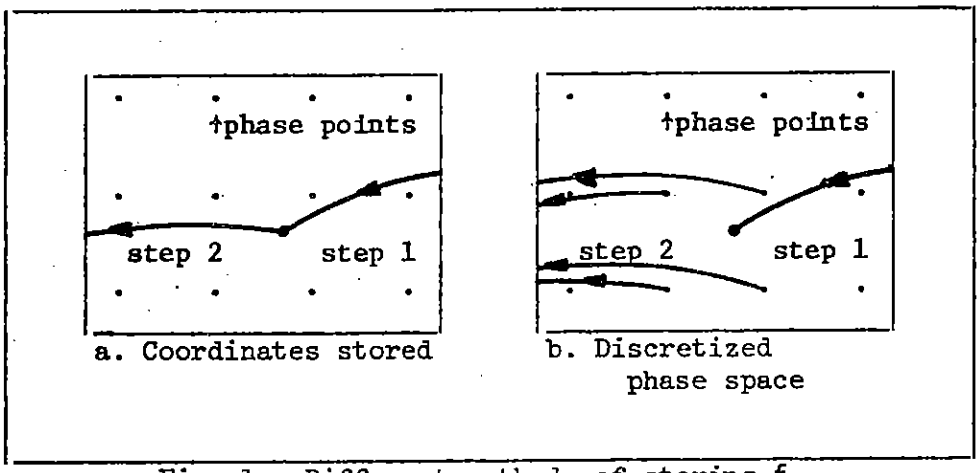

Fig. 1. Different methods of storing f.

Trace Back to an Input Distribution

An altogether different method of evaluating the integral of Eq (14) is to express the distribution function in terms of the known input distribution at the surface. This is the method used by Shankland for steady-state conditions (Ref 8).

In the steady-state case no characteristic curves need be traced. The distribution function is related to the input distribution on the

surface through conservation of energy and angular momentum:

$$f(r,v_r(r),v_\theta) = f_a(a,v_r(a),v_\theta)$$

$$v_r(a) = \sqrt{\frac{-2}{m}\left(V(r) - V(a)\right) + v_r^2(r) + v_\theta^2 \left(\frac{1}{r^2} - \frac{1}{a^2} \right)} \qquad (15)$$

where f_a is the input distribution at the surface radius, a. The potential difference must be consistent with the number of enclosed electrons, N(r).

An even more intuitive approach is possible by using total energy, E, instead of the radial velocity as a coordinate in the distribution function. In this case two coordinates are constants of the motion and

$$f(r,E,v_\theta) = \frac{v_r(a)}{v_r(r)} f_a(a,E,v_\theta) \qquad (16)$$

The factor $v_r(a)/v_r(r)$ is the Jacobian relating the size of volume elements in phase space at the two points. The cooresponding Jacobian in Eq (15) is conveniently equal to one.

The time-dependent case is more complicated. The time a particle left the surface, its creation time, must be known. Also, the total energy of each particle is not constant. The potential energy of a particle changes as $\frac{\partial V(r,t)}{\partial t}$. The distribution cannot be simply related to the input distribution. A characteristic curve must be traced in time through r, v_r, v_θ, t space to the surface, r = a.

Two methods of tracing characteristics back to the surface are worth future investigation. The first is to store the potential function, $V(r,t)$, and use a standard differential equation solver to trace each curve. The major difficulty with this method is excessive computer processing time. Many such curves must be traced to do the triple integration of Eq (14). This integration must be done at each time step in order to extend the potential function. If, through some coordinate transformation to restrict the range of the coordinates, the integral can be done with a seven or nine point integration grid in each coordinate, approximately 500 characteristic curves will have to be traced for each time step. Even more curves may be necessary to obtain accuracy in the dependence of N on r.

The second method of tracing back is to store the endpoints of selected characteristic curves. In addition to the normal coordinates r, v_r, and v_θ one additional coordinate, the creation time, must be stored. The coordinates of the initial point of a characteristic line are specified by location in storage. Since the creation time and v_θ do not change, only two words of memory are necessary, storing r and v_r, to completely determine both endpoints of the line. During each time step, the final points of all curves are moved in a manner identical to the forward time step particle simulation. Values of r, v_r, and v_θ are then chosen to use in the integration, and the value of $f(r,v_r,v_\theta)$ at each point is found by back interpolation. The interpolation is basically three-demensional, as while v_θ remains constant, the creation time must be found. Tracing the particle trajectories forward for one time step rather than

all the way back to their creation should reduce computer time. But the disordered storage of the final r and v_r may make the interpolation process exceedingly difficult. This method requires approximately the same computer core storage as the methods which store f, and it may take more time than the previously discussed method of tracing each curve all the way back to the surface.

IV. Numerical Methods

The method chosen to evaluate the integral of total enclosed charge was to step forward in time and store the distribution function in a discretized phase space. It is physically intuitive and is numerically simple to implement. It has the advantage that physical considerations can be used to make expedient approximations, and to detect blunders. These advantages made this method the choice for a first attempt in the time dependent IEMP program.

The main concern in setting up the numerical system was to keep computer-core and running time to a minimum. The final program used approximately 40K storage (1K=1000 octal) and 120 seconds of CDC 6600 central processing time for a typical run. Extreme accuracy in the results was sacrificed to keep the program from becoming excessively expensive to run. It was designed as a tool to provide coarse results to the time dependent problem. It will provide a basis for comparison with more sophisticated treatments, such as tracing back to the input. If the more sophisticated techniques fail, this method can be refined to produce finer detail in its results. This chapter contains a discussion of the specific techniques used. The program contained a main program and five subroutines, each with a specific purpose. This chapter is organized in a parallel manner.

Main Program

The main program set up the grid of the phase space. A linear grid in all variables was chosen and several different sizes were tried. The final choice was a tradeoff between a fine mesh to give

smooth results, and a rough mesh which would use less computer resources and give faster turnaround time. The final grid chosen contained 9471 points, with the internally scaled integer coordinates varying in the range $0 \le r \le 40$, $-10 \le v_r \le 10$, and $0 \le v_\theta \le 10$. Both core storage and running time varied approximately linearly with the number of points in the grid.

As the program goes through each time step, a subroutine traces the trajectory from each occupied grid point. Another subroutine distributes particles that have landed between grid points to the surrounding grid points. When this has been done for all grid points, the v_r and v_θ integrations of Eq (14) are done as simple sums. The r integration is done by trapezodial rule. New particles are added into the grid for the start of the next time step, and a subroutine is called to compute the potential. The entire process is repeated for each time step.

Tracing and Distributing Particles

Conservation of energy is the basis used to redistribute particles. The energy of the particles does not change during their movement. The trajectory tracing subroutine computes the radial velocity of a particle at each discrete radius through conservation of energy. The time a particle takes to cross from one radius point to the adjacent one is computed from the average of the velocity at the end points. This continues until the period of one time step is used up. Separate loops are provided for particles stopping, turning around, reflecting

off the origin, or doing a combination of these three.

The particle splitting subroutine also is based on conservation of energy. Since angular momentum does not change, the splitting is only two-dimensional. And since the energies associated with the r and v_r coordinates are independent, the splitting can be done independently. Particles need only be placed at the two adjacent coordinates in each variable to conserve energy. By spreading the particles to more points, other properties could be conserved; for example, mean position (Ref 2). But further splitting to conserve other properties would consume computer time and would often require placing negative particles at a point. For these reasons a simple two point split in each coordinate was chosen.

Obtaining Input Distribution

Two subroutines determine the input distribution. The first is used once, at the beginning of the main program. It defines a normalized input distribution, and all the scaling parameters. The program operates in internally defined units. A Maxwellian type of input distribution was used exclusively

$$f_1(v_r,v_\theta) = C_n \int d\phi \; J\left\{\frac{v_y,v_z}{v_\theta,\phi}\right\} \; \exp\left\{-\frac{1}{2}m \; (v_r^2 + v_y^2 + v_z^2) \; / \; T\right\} \qquad (17)$$

where C_n is a normalization factor, T is the equivalent temperature in KeV, and $J\left\{\frac{v_y,v_z}{v_\theta,\phi}\right\}$ is the Jacobian which transforms the units of the distribution function from v_y and v_z to v_θ and ϕ. In the cylindrical case $v_\theta = r \cdot v_y$ and $\phi = v_z$. In the spherical case

$v_\theta = r \cdot \sqrt{v_y^2 + v_z^2}$ and $\phi = \arctan (v_z/v_y)$. The ϕ integration yields a constant in both cases and is absorbed in a new normalization factor. All integrations were done numerically as a matter of convenience.

It must be noted that by introducing this distribution into the system per unit time does not produce a Maxwellian distribution per unit volume in space. The fast particles tend to leave the volume first, so the spatial distribution is more heavily weighted with slow particles. A Maxwllian space distribution could have been produced by multiplying the given input by the total velocity, v.

The velocity scale was hand-fit to this distribution. With the limits of both internal velocities fixed at 10, the v_r velocity scale was set such that a particle with radial velocity 1 has an associated kinetic energy $\frac{1}{32}$ T. The r-scale was set at a $\cdot v_r$-scale. The length of a time step is then computed as r-scale/v_r-scale. Thus a particle with velocity 1 travels a distance 1 in 1 time step.

The input distribution above is applicable to a generating medium where no collisions occur. Since the wall thickness is generally much greater than the free electron range, it is more reasonable to assume that collisions do occur. If a particle is generated at a given distance in the material, it is more likely to escape without a collision when it passes through the minimum amount of material. Thus electrons are more likely to be emitted normal to the surface. This effect produces a cosine dependence identical to the familiar one of optics. In the case of uncharge particles, the cosine dependence will produce a constant number density throughout the cavity,

just as with photon emission. This property provides a check of the numerical procedures.

Other methods of inputting the particles will produce different distributions. If a Maxwellian space-distribution is assumed outside the shell, the distribution of particles crossing the surface per unit time is the Maxwellian times v_r. Since the cosine discussed in the paragraph above is equal to v_r/v, this method of input combines both the cosine and multiplying by v (i.e., $v_r = (v_r/v) \cdot v$). This then is the input distribution which for uncharge particles will produce a uniform Maxwellian space-distribution in the vessel.

A second subroutine is necessary to determine the number of particles emitted per time step. Two such subroutine were used. The steady-state subroutine keeps the current emitted constant. The program runs until the distribution reaches equilibrium. The pulsed subroutine inputs a triangular time pulse, with a linear rise and fall.

Integrating for Potential

Separate subroutines are necessary to compute the potential in spherical and cylindrical coordinates. A trapezodial rule numerical integration is done on Eq (11) or Eq (12), with zero potential assumed at the origin. The units of this potential is made to conform to the program's units. A potential of 1 corresponds to an electron with velocity 1. Recomputing the electric potential at each time step has the effect of changing the total energy of the individual electrons.

V. Numerical Results

Many runs of the program were made. For each run, several specific parameters were input. A vessel radius of 1 meter was chosen in all cases. In time dependent runs, the triangular pulse shape was given a 25 nsec. rise time and 25 nsec. fall time. Most runs were made with the cosine input distribution. Electron temperatures, T, ranged from 1 KeV to 25 KeV, and electron emission, I, ranged from 1 amp/m^2 to 3500 amp/m^2.

The quantities selected for plotting are charge density in coulomb/m^2, and potential in volts (eV for electrons). The charge density is the most widly varying quantity available. Its value is both as a physically interesting result and as graphical display of the coarse grid used. Sample results are given below for several temperatures and emission intensities. All results are for cosine input distribution, unless stated otherwise.

Test Cases

To test the program, the trajectories were computed without the effect of the electric field. Steady-state runs were made with electron temperature 1 KeV and emission 1 amp/m^2. Fig. 2 is a run for the sphere. The theoretical solution is the straight dashed line of charge density $0.024\ 10^{-5}$ coulomb/m^3 in the upper chart. Fig. 3 is the same test for the cylinder.

In both cases, the charge density has a large spike near the origin. The spikes are the result of assigning a large number of

particles zero angular momentum. All these particles can go right through the origin. In reality, these particles have an angular momentum spread from approximately $-\frac{1}{2}$ to $+\frac{1}{2}$ angular momentum units. The large charge density does not, however, greatly affect the potential. The volume is so small near the origin, the total enclosed charge does not appreciably change the computed potential functions. Both potential curves stay close to the theoretical r^2 dependency, and the surface values are within 10% of the theoretical surface values of 4.6 and 6.8 KeV.

The size of the velocity grid limits the possible energy of the particles. The maximum energy of zero angular momentum particles in the grid used here is 3.125 KeV. For steady-state and non-interacting particles, the only quantity which actually changes is the number of electrons emitted per time step. Thus cases with constant $I/\sqrt{T}$ will have the same results. When the electric force is included, cases with equal $I/\sqrt{T}$ will not all behave the same, since the electric potential will be computed in different internally defined units.

Low Temperature and Emission Intensity

The lowest temperature and emission intensity used are the same as in the test cases above; T=1 KeV, I=1 Amp/m^2. Fig. 4 shows the steady-state sphere. The numerically induced spike near the origin is again insignificant in computing the potential. The total potential is 1.25 KeV, which causes the charge density to be higher near the edge.

Fig. 5 shows the sphere with a pulsed input. The 1 amp/m^2 is now the emission at the peak of the triangular pulse. The total charge emitted is the emission integrated over the 25 nsec. rise and 25 nsec. fall: $25 \cdot 10^{-9} \cdot I$. The total potential and total enclosed charge reaches its maximum at 45 nsec. after the start of the pulse.

Similar results occurred for the cylinder. Fig. 6 shows both the steady-state run and the 45 nsec. maximum of the pulsed run.

A disturbing phenomenon occurred at very late times (300 to 1000 nsec.). A small number of particles were apparently trapped in the interior. The last inward-moving electrons are slowed and stopped by the potential caused by other electrons. But when the last group of electrons get near the center, all others have left. The last group loses its energy to the electric field going in, but there is very little field left to push the last group out. Fig. 7 shows the effect at 500 nsec. The 18 eV potential is two orders of magnitude below the earlier values and produces minimal acceleration. The phenomenon is greatly enhanced by assigning many particles zero angular momentum: the $\frac{1}{r^3}$ centrifugal force would generally be much greater than the electric force from 18 Volts.

High Temperature and Emission

The other extrme used was T=25 KeV and I=3500 amp/m^2. The temperature is as high an energy to which this nonrelativistic treatment should be applied. Even at a 25 KeV temperature, the highest velocity particles accounted for are at 78 KeV, well into the relativistic range. The quasi-static assumption also breaks down at

high temperature. The basic time step at 25 KeV is 1.5 nsec., less time than it takes light to cross the 1 meter sphere. The energy of the maximum velocity particles places a limit on the total potential that can be produced by the program.

The results for a steady-state sphere are shown in Fig. 8. Most of the electrons stay near the surface. Only the most energetic can penetrate the strong potential. Pulsed emission gave results nearly idential to the steady-state case. Total potential remained between 65 and 75 KeV through almost all of the pulse, allowing only the most energetic electrons to reach the center. Most electrons were driven out of the vessel with very little penetration, and the change in the emission intensity over the pulse made little difference. In this case, the steady-state charge density with no electric field would be 0.17 10^{-3}coulomb/m^3.

Intermediate Temperature and Emission

Several dozen runs were made with intermediate temperature and emissions. In general, the results for the pulsed input at the pulse peak were very close to the steady-state results. As the temperature and emission intensity are increased, these results become closer. The total potential in the pulsed case occasionally became greater than the steady-state case for brief periods of time. Fig. 9 illustrates a pulsed case where this occurs.

Isotropic Distribution

A few runs were made with isotropic input distributions. Fig. 10

is a steady-state isotropic input for a sphere with the same input parameters as the cosine input in Fig. 4. As expected the charge densities are very similar near the surface, but in the isotropic case the charge density near the center is reduced. In addition, the total potential is lower in the isotropic case.

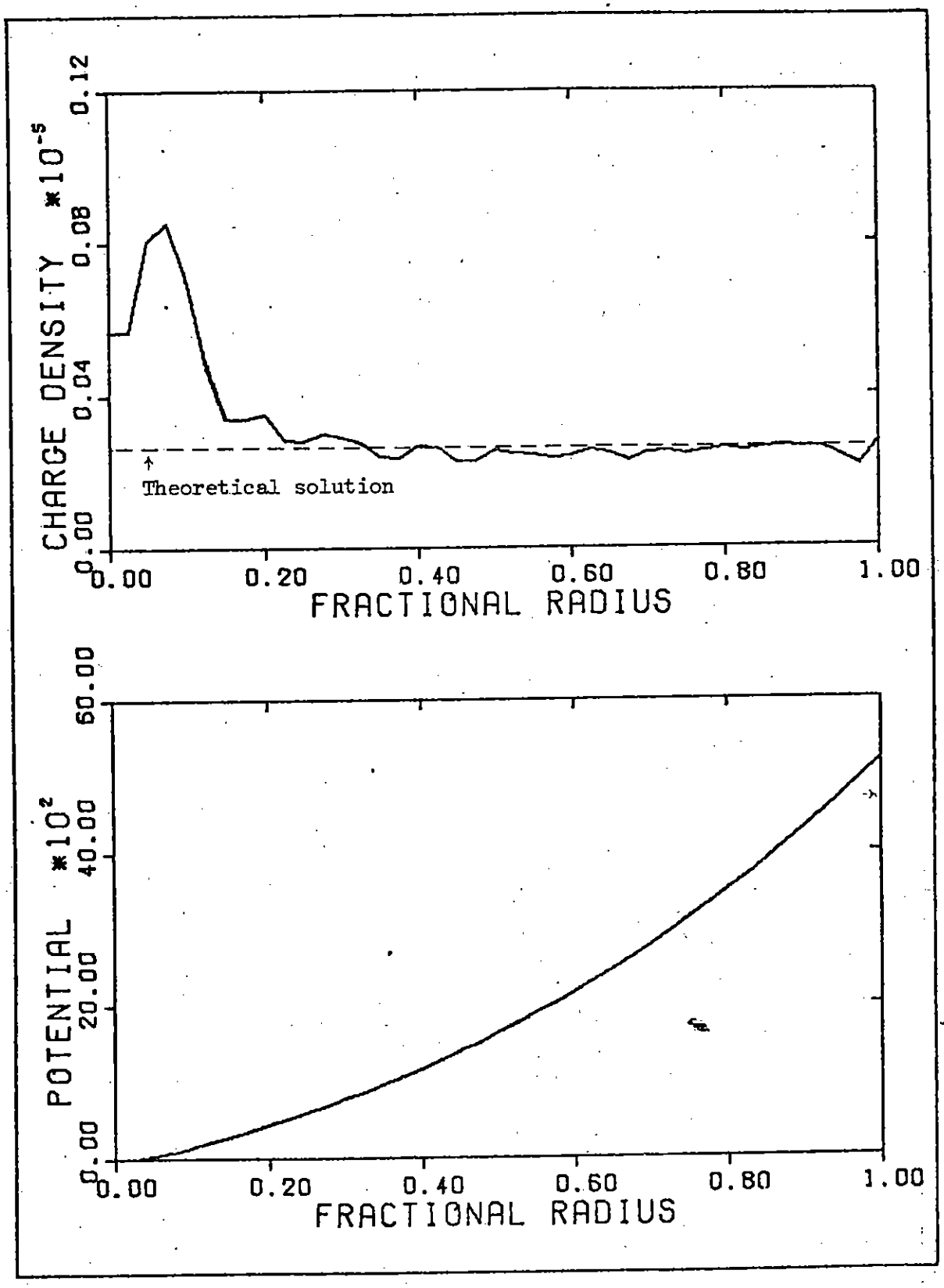

Fig. 2. Sphere; Steady-State; No forces; T=1, I=1

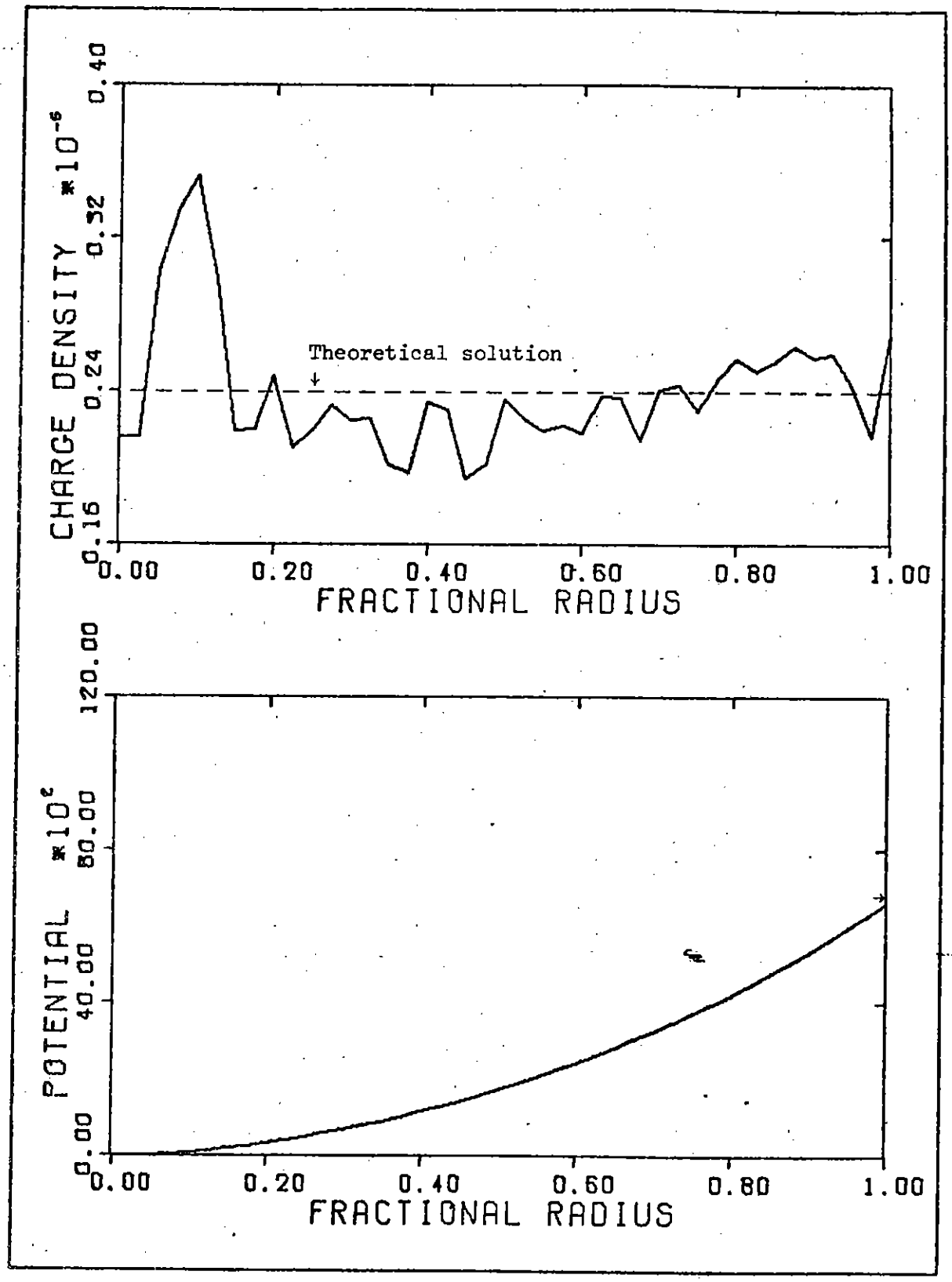

Fig. 3. Cylinder; Steady-State; No Forces; T=1, I=1

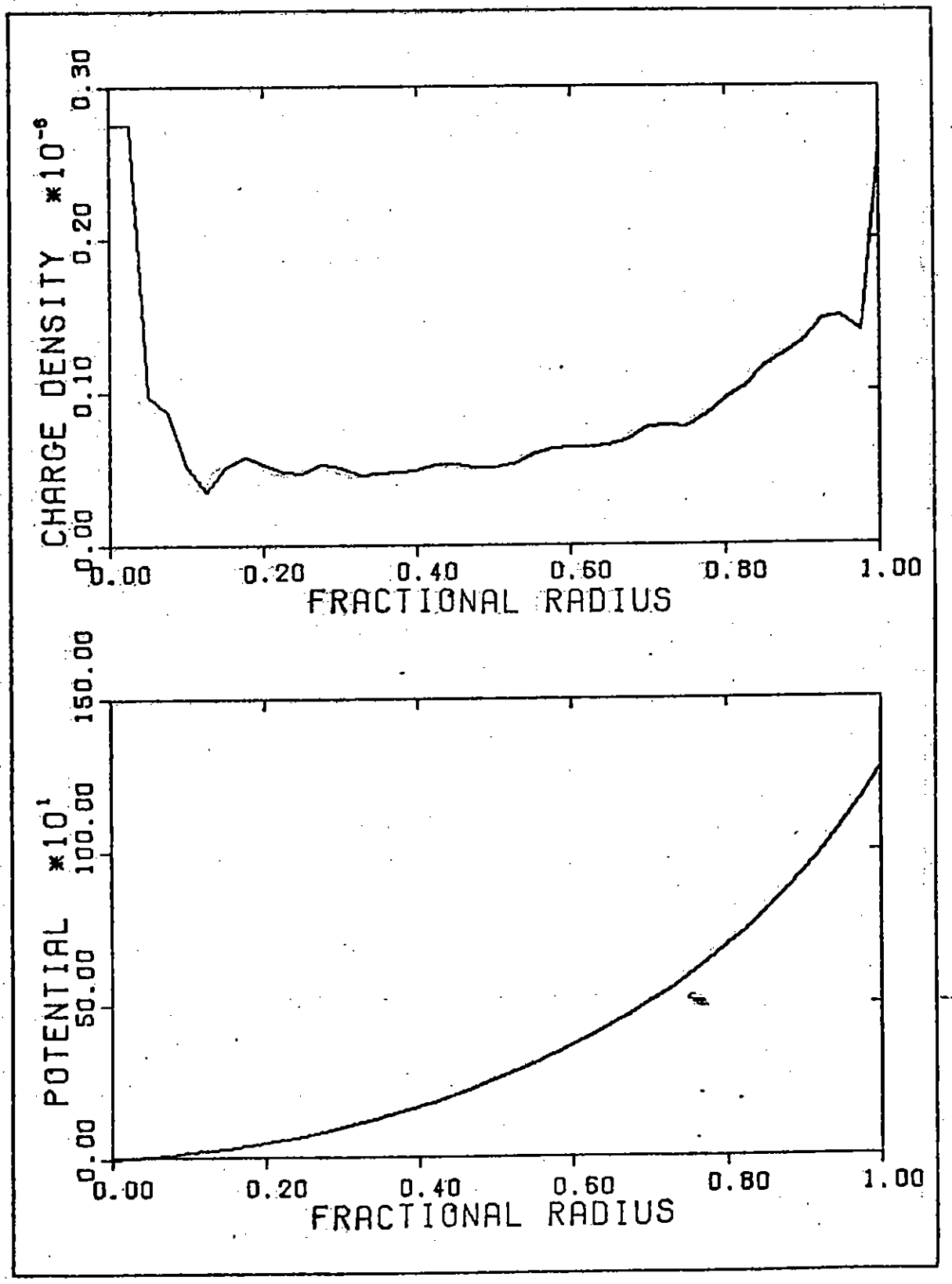

Fig. 4. Sphere; Steady-State; T=1, I=1

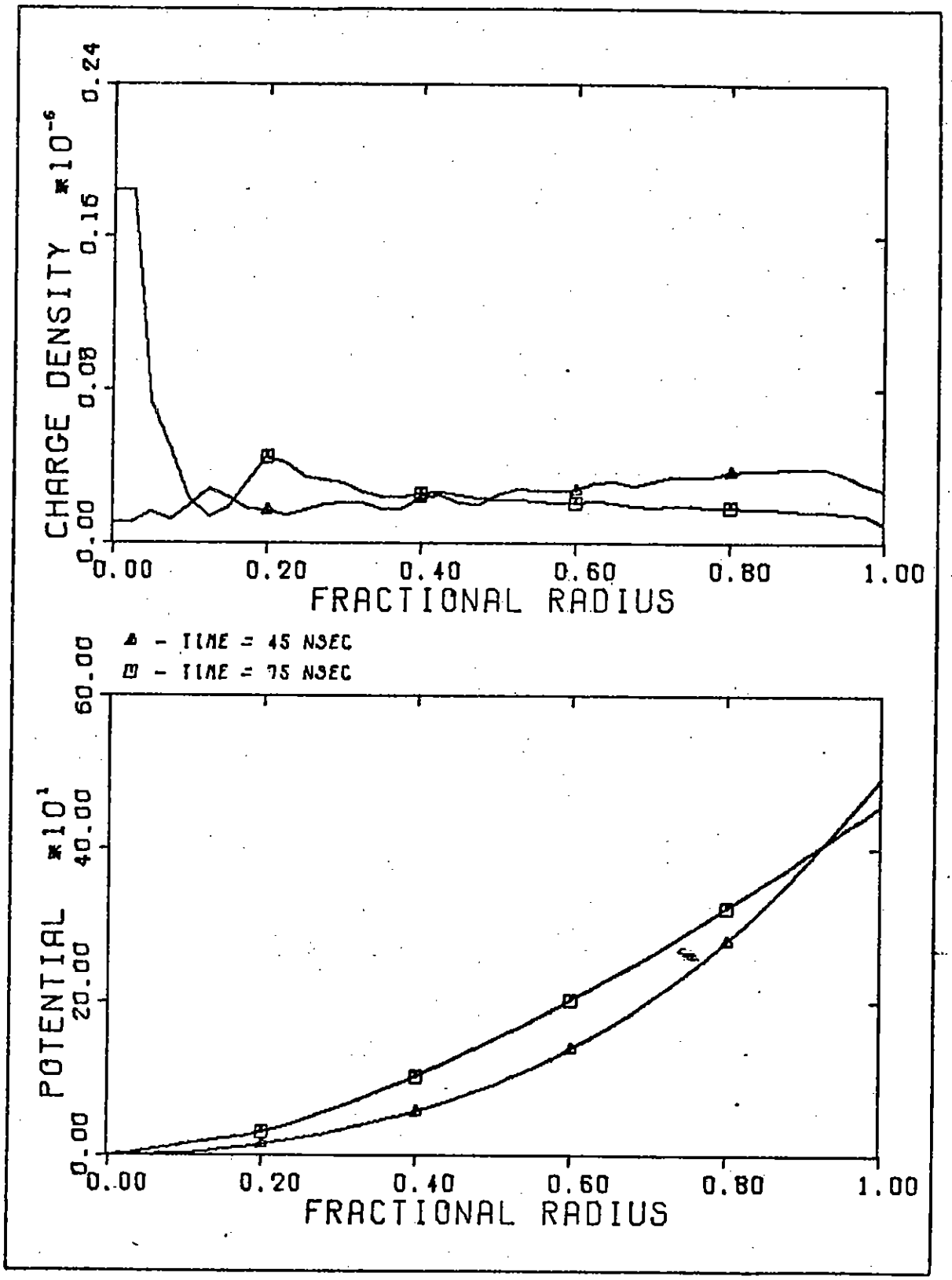

Fig. 5. Sphere; Pulsed: 45 and 75 nsec.; T=1, I=1

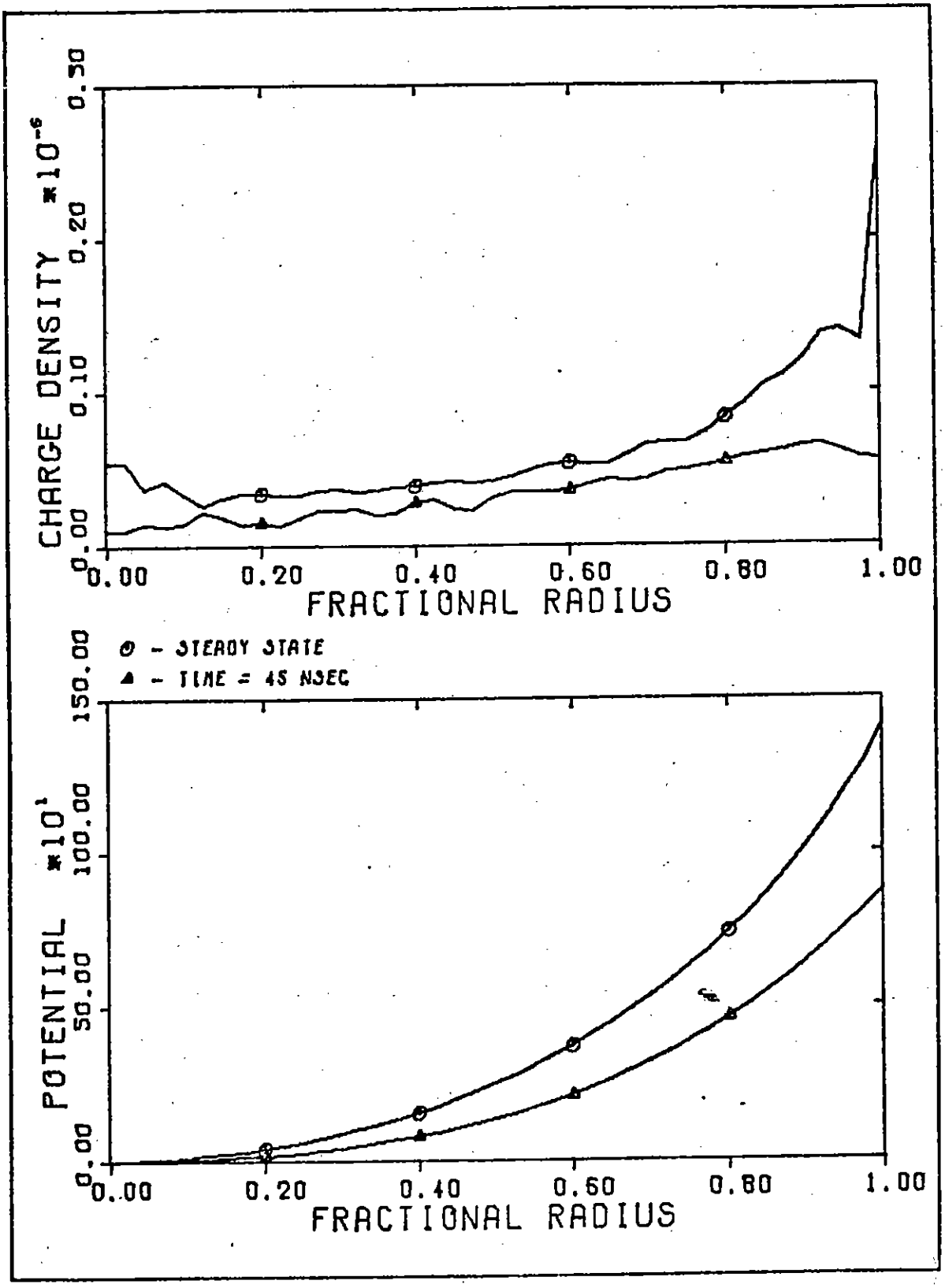

Fig. 6. Cylinder; Steady-State and Pulsed: 45 nsec.; T=1, I=1

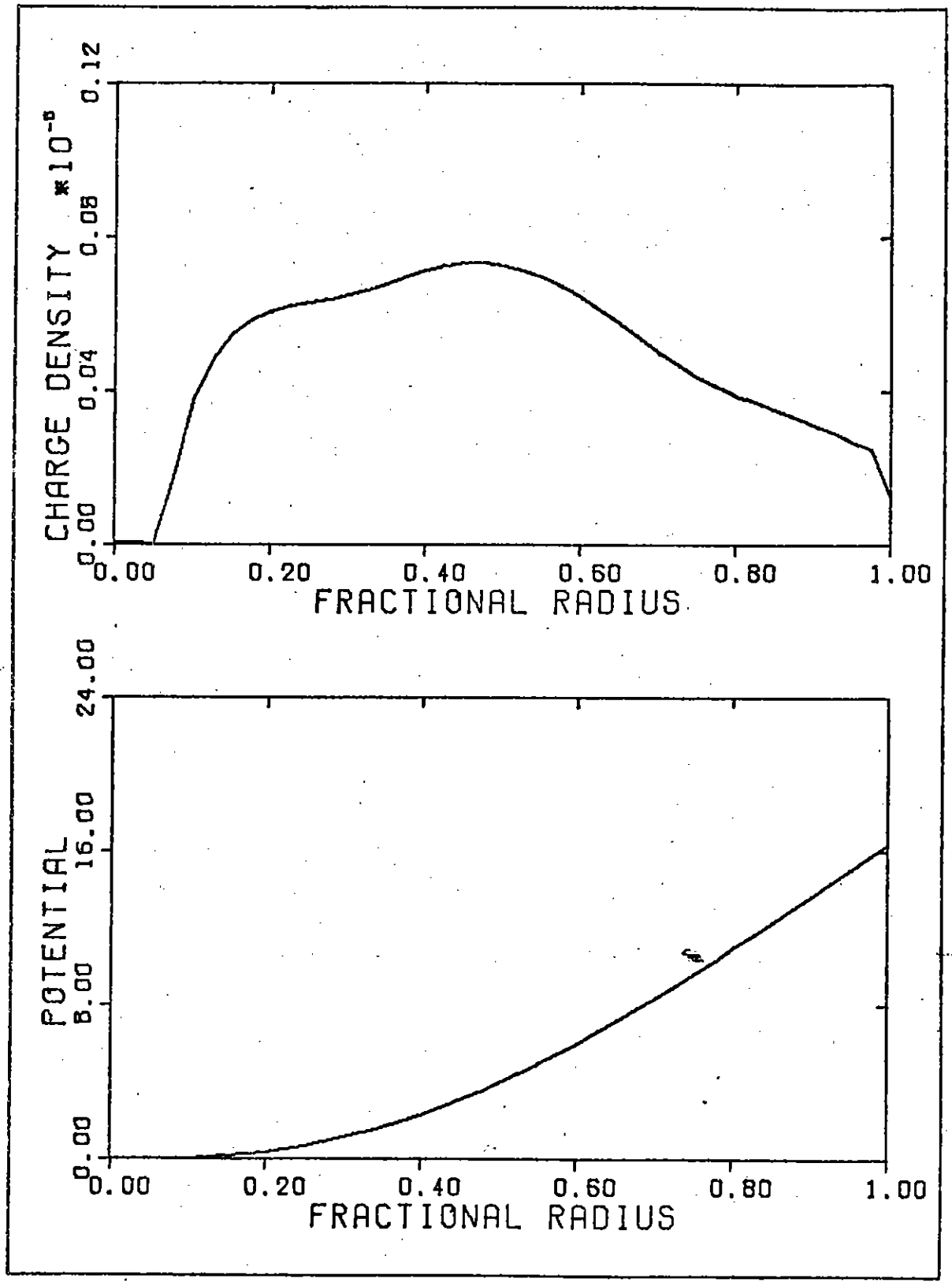

Fig. 7. Cylinder; Pulsed: 500 nsec.; T=1, I=1

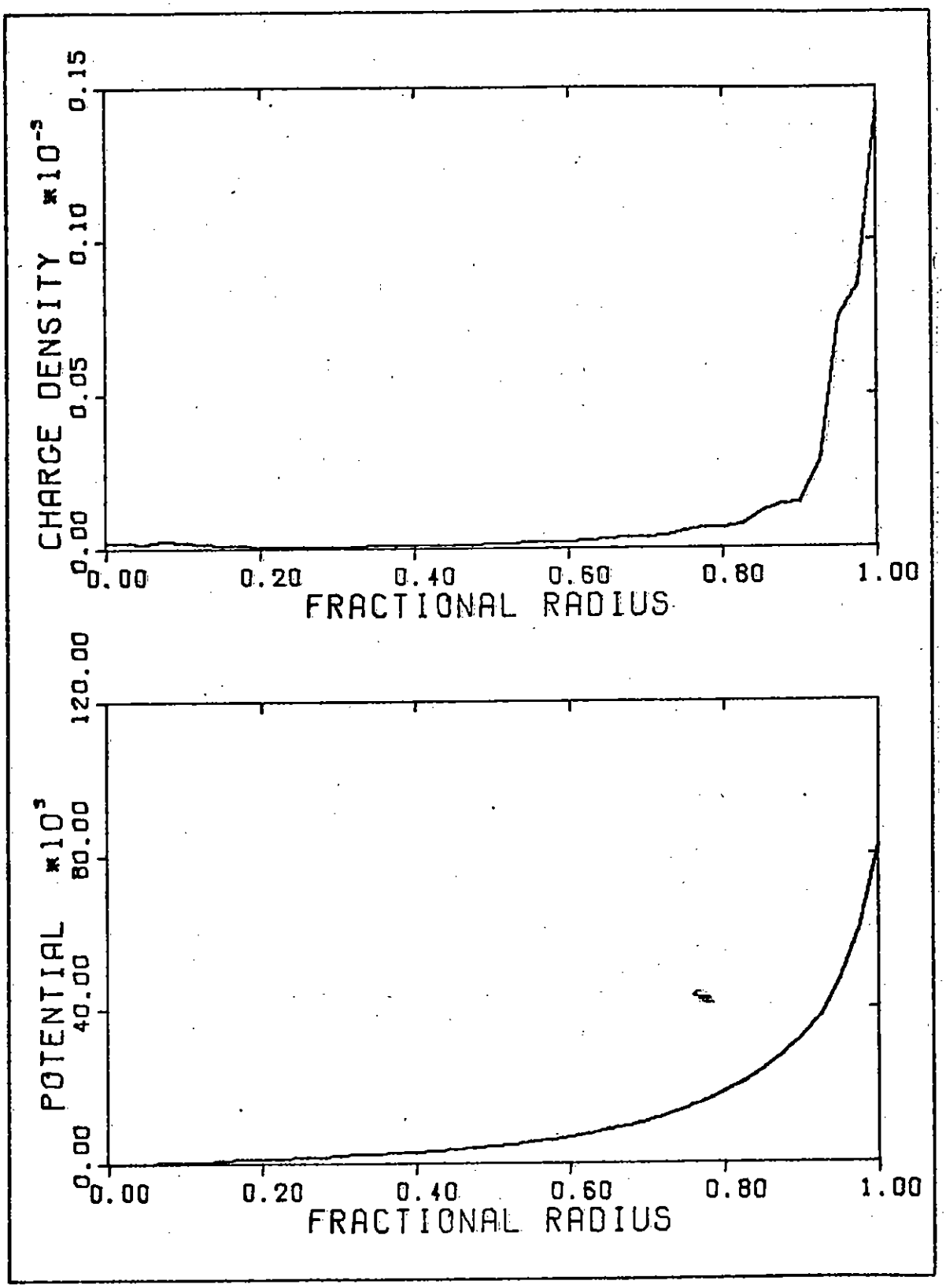

Fig. 8. Sphere; Steady-State; T=25, I=3500

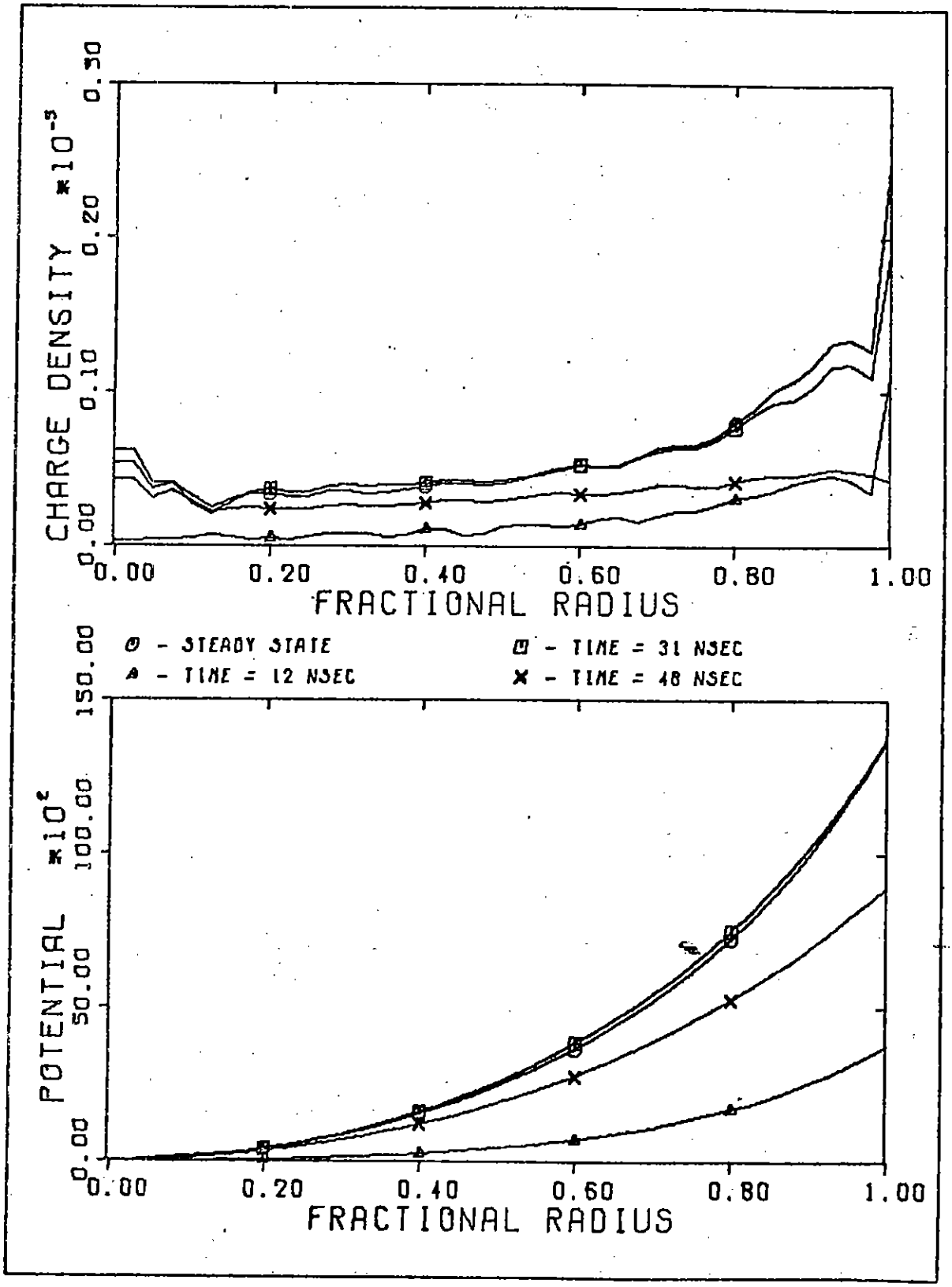

Fig. 9. Cylinder; Steady-State and Pulsed: 12, 31, and 48 nsec.; T=10, I=30

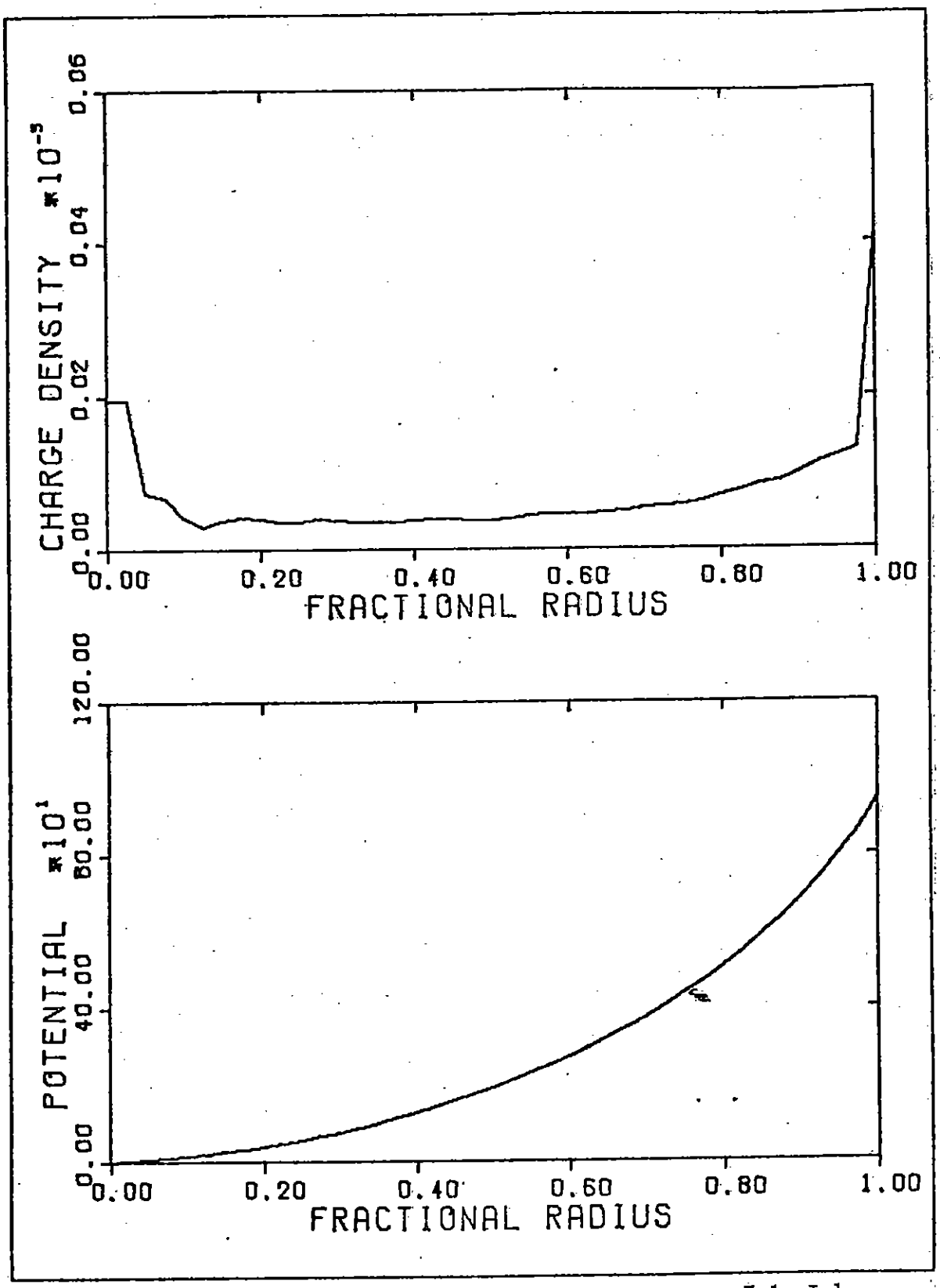

Fig. 10. Sphere; Isotropic Input; Steady-State; T=1, I=1

VI. Conclusions and Recommendations

The primary conclusion of this thesis is that the time-dependent symmetric IEMP problem can be done as a particle simulation without expending large amounts of computer resources. The method worked reasonably well with some limitations. The basic limiting features were:

(a) The coarseness inherent in discretizing the phase space. The upper graph in Figs. 2 through 10 show large point to point fluctuations. The function plotted, charge density, was chosen partly because it shows the fluctuation clearly.

(b) A sizable number of particle were given exactly zero angular momentum. These particles caused inflated charge densities near r=0. The inflated charge density did not have a significant effect on the electric potential. While this problem could have been eliminated by special handling of these particles near r=0, it would not have been worth the additional computer core and running time. Another unrealistic result caused by zero angular momentum particles was their prolonged lingering in the cavity long after the input pulse had ended.

(c) The cutting off of the high energy tail of the distribution caused by the limiting number of the velocity grid points. This cut-off limits the total potential drop from surface to center. New electrons cannot get in to replace old electrons if their input energy is below the potential gap they must cross. In a true Maxwellian distribution, approximately 1% of the particles would have velocities greater than the maximum velocity accounted for here. If the input

emission intensity were high enough, this 1% would cause high enough fields to significantly affect the other 99% of the particles. In a real input energy spectra, however, there will be a cutoff energy, above which there are no particles. If the input distribution were an empirically defined curve with a high energy cutoff, the numerical cutoff would not be a significant limitation.

The next step in the development of this problem should be an attempt to do the time dependent problem by relating back to the input distribution. Two methods of attempting this are discussed in Chapter 3. It is still not known what the computer time and core requirements of either methods will be.

If the problem cannot be efficiently solved by relating back to the input distribution, further development of this particle simulation can be made. The results could be immediately improved by expanding the number of points in the discretized phase space. A nonlinear grid or change of variable for one or more of the phase coordinates might improve the representation of the distribution. In particular, a finer mesh could be used for particles with near zero angular momentum.

Biblography

1. Courant R. and Hibert D. Methods of Matematical Physics, Vol II. New York: Interscience Publishers, 1962.

2. Denavit, J. Numerical Simulation of Plasmas With Periodic Smoothing in Phase Space: NRL Memorandum report 2256, Naval Research Laboratory, Washington, D.C., 1971.

3. Gardner, Robert L. The Electromagnetic Fields Due to Radial Currents Near a Perfectly Conducting Sphere. Unpublished Thesis. Wright-Patterson Air Force Base, Ohio: Air Force Institute of Technology, 1973. DDC #AD753664.

4. Goldstein, H. Classical Mechanics. Reading, Mass: Addison-Wesley Publishing Co., Inc., 1950.

5. Hale, Clovis R. Electric Fields Produced by an Electronic Current Emitted Perpendicular to a Surface. EMP Theoretical note 115. Kirtland Air Force Base, N.M.: Air Force Weapons Laboratory, 1971.

6. Kinsley, Otho V. Introduction to the Electromagnetic Pulse. Unpublished Thesis, Wright-Patterson Air Force Base, Ohio: Air Force Institute of Technology, 1971. DDC #AD735654.

7. Lanczos, C. The Variational Principles of Mechanics (Second Edition). Toronto: University of Toronto Press, 1962.

8. Shankland, D. Spherically Symmetric IEMP Charge and Field Distributions. Unpublished Paper, Wirght-Patterson Air Force Base, Ohio: Air Force Institute of Technology, 1973.

9. Skeem, Marcus R. Electric Fields Generated by Symmetric Inward Emission of Electrons from Cylindrical and Spherical Shells. Unpublished Thesis. Wright-Patterson Air Force Base, Ohio: Air Force Institute of Technology, 1972. DDC #AD753014.

APPENDIX A

Characteristic Curves

Two general views of characteristics are presented here, one algebraic and one geometrical. These are not intended as a rigourous development of the topic. Many texts on partial differential equations offer extensive discussions of the subject (Ref 1:62).

Algebraic View. If u is a function of n variables $x_1, x_2 \ldots, x_n$, the general quasi-linear first order partial differential equation can be written as

$$a_o(x_1, x_2 \ldots, x_n, u) = \sum_1^n a_i(x_1, x_2 \ldots, x_n, u) \frac{\partial u}{\partial x_i} \tag{18}$$

where the coefficients a_i are known functions. We compare this to the total differential of u

$$du = \sum_1^n dx_i \frac{\partial u}{\partial x_i} \tag{19}$$

If we know the value of u and all the $\frac{\partial u}{\partial x_i}$'s at some point, Eq (19) provides a simple means of calculating the value of u in some neighborhood of the point where the partial derivatives remain essentially constant. This is true regardless of the relative magnitude of the dx_i's as long as the dx_i's are small enough to be in the linear region. Unfortunately, in problems such as solving the Vlasov equation, the partial derivatives are not known. But Eq (18) is known to be true. By comparing Eq (18) with Eq (19) we see that if the dx_i's are chosen

equal to the a_i's, then du will equal a_o. The dx_i's can be kept small enough to be in the linear region by dividing Eq (18) by an appropiate constant. Thus by knowning the solution at one point, we can find it at another nearby point and continue the process to trace out a line which is called a characteristic curve.

Geometrical View. To visualize the method geometrically and use ordinary three-space vector analysis, let u be a function of just two variable, x and y. The solution, $u(x,y)$, is and ordinary two dimensional surface, and the basic differential equation can be written

$$a(x,y,u)\cdot p + b(x,y,u)\cdot q = c(x,y,u) \qquad (20)$$

where $p = \frac{\partial u}{\partial x}$ and $q = \frac{\partial u}{\partial y}$. If a point, (x_o,y_o,u_o), is known to be on the solution surface, then at that point a, b, and c are fixed. Eq (20) is now a linear relation between p and q. At that point any solution surface is tangent to be a plane whose orientation can be specified by a vector (p,q,-1) which is normal to the plane. A vector in the line of intersection of any two such planes can be found by taking the cross product of their perpendicular vectors. Doing this and using Eq (20) to eliminate the q's

$$(p_1,q_1,-1) \times (p_2,q_2-1) = \left(\frac{p_1-p_2}{b_0}\right) (a_o,b_o,c_o) \qquad (21)$$

Only the magnitude of this vector depends on the particular planes chosen. The orientation of the vector does not depend on the particular p's and q's chosen but only on the coefficients of Eq (20) at the point. Thus all possible tangent planes to solution surfaces of

Eq (20) will have one line in common. This line defines the characteristic direction and is tangent to a characteristic curve.

To map out the entire solution surface for this case of two independent variables, a one parameter curve must be specified as a boundary condition or initial value. This curve must not be a characteristic curve or all points on it would generate the same characteristic curve, the original one. The curve also must be restricted so as not to produce multiple values of u at any point. These restrictions are not violated in the IEMP problem stated here, and a mathematical discussion of them will be left to the literature.

This geometrical view can be expanded to higher dimensional spaces. The basic Vlasov equation has seven independent variables. Thus its solution is represented by a seven-dimensional surface in an eight-dimensional solution space. To map this surface with characteristic curves, the curves must originate from a six-dimensional boundary condition.